Journal of Solid State Chemistry 181 (2008) 2523–2529

Contents lists available at ScienceDirect

Journal of Solid State Chemistry

journal homepage: www.elsevier.com/locate/jssc

Crystal structures and chemistry of double perovskites $Ba_2M(II)M'(VI)O_6$ (M = Ca, Sr, M' = Te, W, U)

W.T. Fu *, Y.S. Au, S. Akerboom, D.J.W. IJdo

Leiden Institute of Chemistry, Gorlaeus Laboratories, Leiden University, P.O. Box 9502, 2300 RA Leiden, The Netherlands

ARTICLE INFO

Article history:
Received 21 December 2007
Received in revised form
22 May 2008
Accepted 7 June 2008
Available online 17 June 2008

Keywords:
Perovskite
X-ray powder diffraction
Neutron powder diffraction
Crystal structure
Phase transition

ABSTRACT

Structures of the double perovskites $Ba_2M(II)M'(VI)O_6$ (M = Ca, Sr, M' = Te, W, U) at room temperature have been investigated by the Rietveld method using X-ray and neutron powder diffraction data. For double perovskites with M = Sr, the observed space groups are $I2/m$ (M' = W) and $R\bar{3}$ (M' = Te), respectively. In the case of M = Ca, the space groups are either monoclinic $P2_1/n$ (M' = U) or cubic $Fm\bar{3}m$ (M' = W and Te). The tetragonal and orthorhombic symmetry reported earlier for Ba_2SrTeO_6 and Ba_2CaUO_6, respectively, were not observed. In addition, non-ambient X-ray diffraction data were collected and analyzed for Ba_2SrWO_6 and Ba_2CaWO_6 in the temperature range between 80 and 723 K. It was found that the rhombohedral $R\bar{3}$ structure exists in Ba_2SrWO_6 above room temperature between the monoclinic and the cubic structure, whereas the cubic Ba_2CaWO_6 undergoes a structural phase transition at low temperature to the tetragonal $I4/m$ structure.

1. Introduction

Quaternary perovskites with the general formula $A_2MM'O_6$ usually adopt the 1:1 ordering of the M and M' cations if a large difference exists in either their charge or ionic radii. These so-called double perovskites attract considerable attention as they exhibit interesting structural and physical properties. For example, the monoclinic double perovskite $Ba_2Bi(III)Bi(V)O_6$ is the parent compound of the superconducting systems $BaBi_{1-x}Pb_xO_3$ [1] and $Ba_{1-x}K_xBiO_3$ [2], which have the maximum transition temperature (T_c) of about 12 and 35 K, respectively. On the other hand, some ordered double perovskites are interesting candidates for microwave dielectric resonators widely used in today's telecommunication systems [3,4]. Moreover, it has been shown that the Sr_2FeMoO_6 exhibits magnetoresistive effect well above room temperature [5].

The ideal double perovskites $A_2MM'O_6$ have a cubic symmetry with the space group $Fm\bar{3}m$. This symmetry is usually expected when the tolerance factor

$$t = \frac{(r_A + r_O)}{\sqrt{2}(\bar{r}_{(M,M')} + r_O)}$$

where $\bar{r}_{(M,M')}$ is the averaged ionic radius of the M and M' cations, is close to unity. For the majority of double perovskites, however, the size of the A-cation is too small to fit in the cavity formed by the 12 anions. In such case, the tilting of octahedra generally occurs leading to a lower symmetry. Woodward [6] has, based on the Glazer's [7] classification of the tilt systems, derived 13 possible space groups for double perovskites by considering the cationic ordering and the rotation of octahedra occurring simultaneously. Howard et al. [8] undertook a group-theoretical analysis, identifying 12 space groups under the same conditions.

Recently, we have systematically investigated the room temperature structures of several double perovskites with the formula $Ba_2Ln(III)M(V)O_6$ (Ln = lanthanides and Y and M = Ru, Ir, Sb, and Nb) in relation with their tolerance factors (t) [9–12]. Although the tolerance factor values at the boundary of the phase transition may vary, the above-mentioned double perovskites show the following trends: (i) The cubic $Fm\bar{3}m$ structure occurs with the tolerance factor t being above about 0.98. (ii) When t is approximately between 0.96 and 0.98, the double perovskites adopts either the rhombohedral $R\bar{3}$ (tilt system $a^-a^-a^-$) or the tetragonal $I4/m$ (tilt system $a^0a^0c^-$) structure depending on the covalency of the pentavalent cations [12]. (iii) For compounds with lower t, the monoclinic tilt system $a^0b^-b^-$ ($I2/m$) is favoured. (iv) All tilt systems occurred in $Ba_2Ln(III)M(V)O_6$ contain only the out-of-phase tilting of the octahedra about the two-, three- and four-fold axis of the cubic aristotype.

Related to these studies, it is of interest to look for the structures that occur in the double perovskite family $Ba_2M(II)M'(VI)O_6$ with even larger variable tolerance factors. The structural details are known for some of them. For example, Ba_2SrUO_6 [13] adopts the space group $P2_1/n$ (tilt system $a^-a^-c^+$) as

* Corresponding author. Fax: +31 71 5274537.
E-mail address: w.fu@chem.leidenuniv.nl (W.T. Fu).

0022-4596/$ - see front matter © 2008 Elsevier Inc. All rights reserved.
doi:10.1016/j.jssc.2008.06.024

was derived from the neutron powder diffraction data. Ba_2SrIrO_6 and Ba_2CaIrO_6 were reported to have the space group $R\bar{3}m$ and $Fm\bar{3}m$ [14], respectively. The results for other compounds are, however, either lacking or in conflict. Steward and Rooksby [15] found Ba_2SrWO_6 deviating moderately from cubic symmetry at room temperature and becoming cubic at approximately 773 K. Kovba et al. [16] described it as monoclinic at room temperature. Cox et al. [17] have, using synchrotron X-ray diffraction, determined the space group of Ba_2SrWO_6 to be $I2/m$, without giving the atomic positions. Recently, Khalyavin et al. [18] have refined the structure of Ba_2SrWO_6 in the triclinic space group $F\bar{1}$. The double perovskite Ba_2SrTeO_6 has been reported to be tetragonal with the cell dimension of $a = b \approx 2a_p$ and $c \approx 2a_p$, where a_p is the lattice parameter of the primitive cubic aristotype [19]. Kemmler-Sack and Seemann [20] found that Ba_2CaUO_6 has an orthorhombic unit cell with $a = 6.154$ Å, $b = 6.124$ Å, and $c = 8.643$ Å. The same compound was also described as a slightly distorted cubic perovskite with $a = 8.669(4)$ Å [21]. No structural details have yet been reported for both Ba_2SrTeO_6 and Ba_2CaUO_6. Finally, Ba_2CaWO_6 was reported by Steward and Rooksby [15], Filip'ev et al. [22], and Chiu and Bauer [23] to be cubic ($Fm\bar{3}m$). Very recently, Yamamura et al. [24] have studied the structures of the double perovskites Ba_2CaMO_6, M = W, Re, and Os. While the compounds with M = Re and Os adopt the space group $Fm\bar{3}m$, Ba_2CaWO_6 was found to be tetragonal at room temperature with the space group $I4/m$. They also observed a second-order phase transition at $T \approx 220$ K and assigned the transition to be $I4/m \rightarrow I2/m$.

In a recent publication [25], we reported the crystal structures of the double perovskites $Ba_2Sr_{1-x}Ca_xWO_6$ based on the X-ray diffraction study. The structure of the end members was confirmed to be either monoclinic ($I2/m$) or cubic ($Fm\bar{3}m$), with $x = 0$ and 1, respectively. We also observed the existence of the rhombohedral $R\bar{3}$ structure in the solid solution. In the present studies, we have investigated the room temperature structures of three double perovskites, i.e. Ba_2SrTeO_6, Ba_2CaUO_6, and Ba_2CaTeO_6. Non-ambient X-ray diffraction was also carried out to examine whether there exists an intermediate structure in Ba_2SrWO_6 between the monoclinic and the cubic structure [15] as well as the nature of the low temperature structure of Ba_2CaWO_6 [24]. We report the new findings in this paper.

2. Experimental

Samples of $Ba_2MM'O_6$ (M = Ca, Sr; M' = Te, W, and U) were prepared from $BaCO_3$, $SrCO_3$, $CaCO_3$, TeO_2, WO_3, and U_3O_8 in alumina crucibles using the standard solid-state reaction. Due to the low melting point of TeO_2, these mixtures were first heated at 600 °C overnight. The resultant powders were then sintered with a temperature step of 100 °C and 20 h at each step with regrinding. The final sintering temperature was 1100 °C for the Te compounds and 1300 °C for the other compounds. All syntheses were carried out in air and finished by furnace-cooling to room temperature.

X-ray diffraction data at room temperature were collected with a Philips X'Pert diffractometer equipped with the X'celerator using Cu$K\alpha$ radiations. For non-ambient X-ray diffraction, an Anton Paar TTK 450 chamber with the direct sample cooling/heating in the temperature range between 80 and 723 K and a temperature stability of <0.2 K. The neutron powder diffraction data were obtained at room temperature for Ba_2CaUO_6 and Ba_2SrWO_6 on the powder diffractometer of the High-Flux Reactor of NRG in Petten, with the neutron wavelength of 1.433 Å and in steps of 0.1° (2θ). A vanadium can was used as sample holder. The scattering lengths used in the calculations are $b_{(Ba)} = 5.07$, $b_{(Ca)} = 4.70$, $b_{(Sr)} = 7.02$, $b_{(W)} = 4.77$, $b_{(U)} = 8.417$, and $b_{(O)} = 5.803$ fm. Since the neutron absorption cross-section for these elements are relatively small, no absorption corrections were made.

The calculations were performed by the profile analysis of the Rietveld method using the Rietica computer program [26].

3. Results

X-ray powder diffraction patterns of all $Ba_2MM'O_6$ (M = Ca, Sr; M' = Te, W, and U) samples show strong lines characteristic of the primitive perovskite structure. However, the line splitting is clearly visible in some of them, which suggests the true symmetry being lower than cubic. In addition, the presence of superlattice reflections, e.g. $2\theta \approx 18°$ and 35°, with substantial intensity indicates the ordered arrangement of the alkaline earth and hexavalent cations. To determine the correct symmetries and the associated space groups of the double perovskites, we examined both the splitting of the basic reflections of the primitive cubic perovskite and the occurrence of superlattice reflections.

In Fig. 1, the enlarged sections containing the basic (222) and (400) reflections of the cubic aristotype are shown. For Ba_2SrWO_6 and Ba_2CaUO_6, the (222) reflection splits in a triplet and the (400) reflection splits in a doublet. This is readily explained by a monoclinic distortion. Confirming our recent X-ray diffraction study [25], the neutron powder diffraction data of Ba_2SrWO_6 shows that all observed superlattice reflections are indexed with the odd–odd–odd indices in terms of a double-edged unit cell (see Fig. 4). This indicates that only out-of-phase tilting is possible in this compound, and the space group $I2/m$ is a logical choice [6,8]. In Ba_2CaUO_6, besides the odd–odd–odd super reflections, several very weak lines with the even–even–odd indexing are also visible in both X-ray and neutron powder diffraction pattern (see Fig. 4). The additional superlattice reflections arise from the in-phase tilt of the octahedra. Consequently, the likely space group is $P2_1/n$. For Ba_2SrTeO_6, the basic (222) reflection is a doublet with the intensity ratio of about 3:1; the basic (400) reflection does not split (Fig. 1). This is characteristic of a rhombohedral symmetry. Since the observed superlattice reflections in Ba_2SrTeO_6 correspond to the out-of-phase tilting of the octahedra, the space group

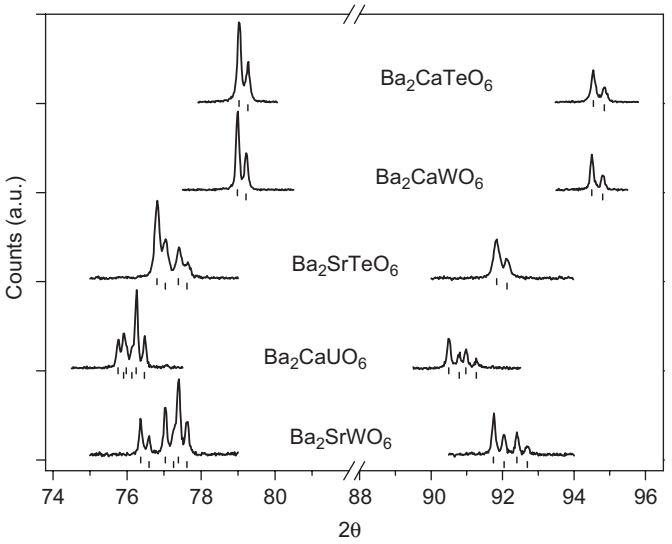

Fig. 1. An enlarged section of the X-ray diffraction patterns of $Ba_2MM'O_6$ (M = Sr, Ca, M' = U, W, Te) showing the basic (222) and (400) reflections. The tick marks below are the calculated positions of Bragg's reflections using the refined lattice parameters of the corresponding space groups. The significance of the peak splitting due to the octahedral tilting is discussed in the text.

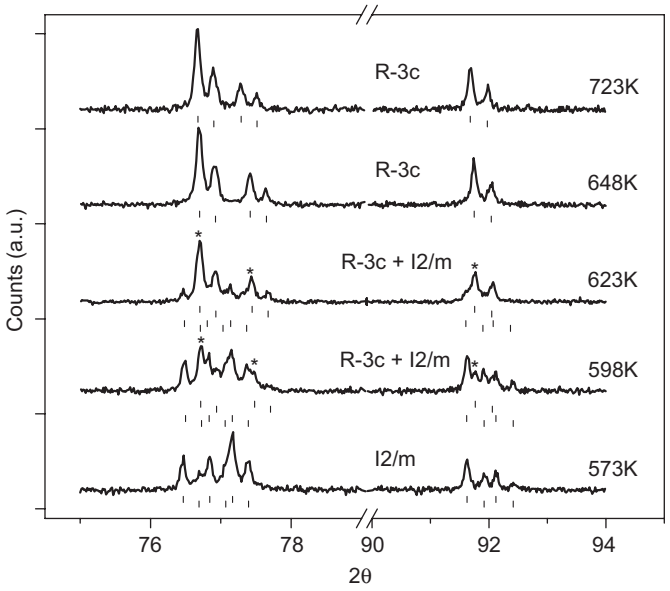

Fig. 2. A section of the X-ray diffraction patterns of Ba_2SrWO_6 showing the evolution of the basic (222) and (400) reflections as the function of temperature. The existence of two-phase region can be clearly seen by the progressive increase of the rhombohedral $R\bar{3}$ phase marked by asterisk (*).

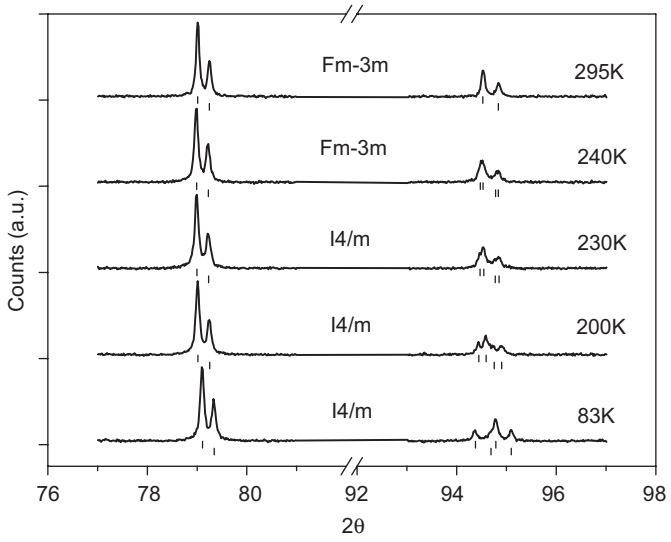

Fig. 3. A section of the X-ray diffraction patterns of Ba_2CaWO_6 showing the evolution of the basic (222) and (400) reflections as the function of temperature.

$R\bar{3}$ is evident. Finally, we did not observe any peak splitting in both Ba_2CaWO_6 and Ba_2CaTeO_6, indicating that these compounds adopt the cubic space group $Fm\bar{3}m$.

The structures that occur in Ba_2MWO_6 (M = Sr and Ca) at non-ambient temperature were analyzed in the same way. In the case of Ba_2SrWO_6, no occurrence of additional reflections that may suggest the $I2/m \rightarrow P2_1/n$ phase transition was seen on cooling down to 80 K. However, since the compound contains heavy atoms, the intensity of the superlattice reflections associated with the in-phase tilting may be extremely weak to be revealed by X-ray diffraction technique. On the other hand, examination of X-ray diffraction patterns at high temperature has clearly revealed a phase transition (Fig. 2). At 648 K, the triplet of the basic (222) reflection becomes a doublet and the splitting of the basic (400) reflection disappears. This is typical of rhombohedral symmetry of the space group $R\bar{3}$(see also Fig. 1 for Ba_2SrTeO_6). It is also observed that the $I2/m \rightarrow R\bar{3}$ phase transition shows hysteresis and exhibits a two-phase region in the temperature range of about 598–623 K. The rhombohedral structure persists till 723 K, the highest temperature being reachable with the TTK 450 chamber. For Ba_2CaWO_6, a different phase transition occurs (Fig. 3). At $T = 240$ K, the basic (400), though not yet split, becomes visibly broad, whereas the basic (222) reflection remains unchanged. The splitting of (400) reflection begins visible at $T = 230$ K. As there are no superlattice reflections arising from in-phase tilting of the adjacent octahedra, the space group $I4/m$ is a logical choice [6,8]. The tetragonal distortion increases with decreasing temperature. No further structural change was observed down to 80 K.

The structures of the double perovskites $Ba_2M(II)M'(VI)O_6$ (M = Ca, Sr, M' = Te, W, U) were modeled in the above-mentioned space groups. For Ba_2SrWO_6 and Ba_2CaUO_6, the refinements of the room temperature structure were carried out using combined neutron and X-ray diffraction data. All refinements yielded the satisfactory results. The refined crystallographic data are listed in Tables 1–3. Plots of the observed and calculated profiles of some representative compounds are shown in Fig. 4.

4. Discussion

4.1. Ba_2SrWO_6

The structure determination of Ba_2SrWO_6 using combined neutron and X-ray diffraction data confirms once again the space group $I2/m$ as was originally reported by Cox et al. [17] and is in agreement with the lattice parameters given by Kovba et al. [16]. There is no evidence to suggest the triclinic space group $F\bar{1}$ [18]. The structure of Ba_2SrWO_6 can be derived from the cubic aristotype by ordering the Sr(II) and W(VI) cations and by tilting the SrO_6/WO_6 octahedra about the [110]-axis. The tilt system $a^-a^-c^0$ is consistent with Ba_2SrWO_6 as the tolerance factor ($t = 0.929$) deviates largely from unity. In fact, the space group $I2/m$ has also been observed in a number of double perovskites, e.g. $Ba_2Bi(III)Bi(V)O_6$ ($t = 0.927$) [27], Ba_2LnBiO_6, Ln = Pr and Nd ($t = 0.936$ and 0.937) [28] and Ba_2LnNbO_6 (Ln = La, Pr, Nd, and Sm with t between 0.956 and 0.968) [12], all with relatively small tolerance factors.

The monoclinic structure survives until the temperature of about 573 K. As the temperature increases further, the rhombohedral $R\bar{3}$ structure appears across a two phase region of approximately 50 K. The coexistence of two phases close to the phase transition temperature is characteristic of a first-order phase transition, and has also been observed in perovskites with the similar phase transition between the $a^-a^-c^0$ and $a^-a^-a^-$ tilt systems [29] or between the $a^-a^-c^0$ and $a^0a^0c^-$ tilt systems [30]. The occurrence of the rhombohedral structure in Ba_2SrWO_6 as the function of temperature is the same as that observed in $Ba_2Sr_{1-x}Ca_xWO_6$ by changing the composition [25]. It demonstrates that the direct phase transition between the $a^-a^-c^0$ and $a^-a^-a^-$ tilt systems is unlikely to occur, though such a transition has been reported in the $Ba_{2-x}Sr_xLuBiO_6$ system [31]. As was mentioned above, Steward and Rooksby [15] have observed Ba_2SrWO_6 becoming cubic at approximately 773 K. Although the highest temperature of present investigation was limited to 723 K, it is unlikely that the cubic symmetry will occur at ~773 K. This can be seen from the refined rhombohedral angle at 723 K (Table 2), which still differs largely from 60°. In fact, the refined α-values, e.g. 60.391° (648 K), 60.377° (673 K), 60.361° (698 K), and 60.347° (723 K), decreases linearly with increasing temperature leading to the fit: $\alpha = 60.772 - 5.88 \times 10^{-4}T$. If one suggests that the

Table 1
Refined lattice parameters and atomic positions of $Ba_2MM'O_6$ (M = Sr, Ca, M' = U, W, Te) at room temperature

Ba_2SrWO_6 *I2/m*		Ba_2SrTeO_6 *R*$\bar{3}$		Ba_2CaUO_6 *P*$2_1/n$		Ba_2CaWO_6 *Fm*$\bar{3}m$		Ba_2CaTeO_6 *Fm*$\bar{3}m$	
a (Å)	6.10677(6)	*a* (Å)	6.05660(6)	*a* (Å)	6.16146(7)	*a* (Å)	8.39405(3)	*a* (Å)	8.39460(6)
b (Å)	6.03732(8)	*α* (deg)	60.342(1)	*b* (Å)	6.11877(7)				
c (Å)	8.5399(1)			*c* (Å)	8.6975(1)				
β (deg)	90.4457(7)			*β* (deg)	90.1005(8)				
Ba	4*i* (*x*,0.5,*z*)	Ba	2*c* (*x*,*x*,*x*)	Ba	4*e* (*x*,*y*,*z*)	Ba	8*c* (0.25,0.25,0.25)	Ba	8*c* (0.25,0.25,0.25)
x	0.4951(3)	*x*	0.2506(1)	*x*	0.4966(5)	*B* (Å)^2	0.43(2)	*B* (Å)^2	0.43(1)
z	0.2500(2)	*B* (Å)^2	0.57(2)	*y*	0.4880(2)	Ca	4*a* (0,0,0)	Ca	4*a* (0,0,0)
B (Å)^2	0.38(3)	Sr	1*a* (0,0,0)	*z*	0.2496(2)	*B* (Å)^2	0.79(7)	*B* (Å)^2	0.44(5)
Sr	2*c* (0.5,0,0)	*B* (Å)^2	0.68(3)	*B* (Å)^2	0.46(2)	W	4*b* (0.5,0.5,0.5)	Te	4*b* (0.5,0.5,0.5)
B (Å)^2	0.18(4)	Te	1*b* (0.5,0.5,0.5)	Ca	2*d* (0.5,0,0)	*B* (Å)^2	0.09(2)	*B* (Å)^2	0.13(2)
W	2*b* (0,0.5,0)	*B* (Å)^2	0.26(1)	*B* (Å)^2	1.09(9)	O	24*e* (*x*,0,0)	O	24*e* (*x*,0,0)
B (Å)^2	0.12(3)	O	6*f* (*x*,*y*,*z*)	U	2*c* (0,0.5,0)	*x*	0.2656(4)	*x*	0.2669(6)
O(1)	4*i* (*x*,0,*z*)	*x*	0.267(2)	*B* (Å)^2	0.06(1)	*B* (Å)^2	1.81(1)	*B* (Å)^2	0.62(8)
x	0.5620(7)	*z*	0.233(1)	O(1)	4*e* (*x*,*y*,*z*)				
z	0.2765(5)	*z*	0.307(1)	*x*	0.215(2)				
B (Å)^2	0.91(14)	*B* (Å)^2	0.84(4)	*y*	0.235(2)				
O(2)	8*j* (*x*,*y*,*z*)			*z*	0.035(2)				
x	0.2189(4)			*B* (Å)^2	0.60(48)				
y	0.2765(6)			O(2)	4*e* (*x*,*y*,*z*)				
z	0.0342(3)			*x*	0.251(2)				
B (Å)^2	1.04(8)			*y*	0.723(2)				
				z	0.028(2)				
				B (Å)^2	0.95(46)				
				O(3)	4*e* (*x*,*y*,*z*)				
				x	0.576(1)				
				y	0.012(2)				
				z	0.267(1)				
				B (Å)^2	0.65(22)				
R_{wp} = 4.20%[a] (11.27%[b])		R_{wp} = 12.41%[b]		R_{wp} = 3.85%[a] (16.85%[b])		R_{wp} = 10.63%[b]		R_{wp} = 15.89%[b]	
R_p = 3.27%[a] (8.63%)[b]		R_p = 8.72%[b]		R_p = 3.00%[a] (13.13%)[b]		R_p = 7.71%[b]		R_p = 11.20%[b]	

[a] *R*-values of neutron data.
[b] *R*-values of the X-ray data.

Table 2
Refined lattice parameters and atomic positions of Ba_2SrWO_6 and Ba_2CaWO_6 at non-ambient temperature

Ba_2SrWO_6						Ba_2CaWO_6			
T = 523 K *I2/m*		*T* = 648 K *R*$\bar{3}$		*T* = 723 K *R*$\bar{3}$		*T* = 83 K *I*4/*m*		*T* = 200 K *I*4/*m*	
a (Å)	6.10462(5)	*a* (Å)	6.05456(5)	*a* (Å)	6.05996(4)	*a* (Å)	5.92270(3)	*a* (Å)	5.93033(3)
b (Å)	6.05096(5)	*α* (deg)	60.3903(9)	*α* (deg)	60.3474(9)	*c* (Å)	8.40360(5)	*c* (Å)	8.39684(7)
c (Å)	8.55781(7)								
β (deg)	90.2715(7)								
Ba	4*i* (*x*,0.5,*z*)	Ba	2*c* (*x*,*x*,*x*)	Ba	2*c* (*x*,*x*,*x*)	Ba	4*d* (0,0.5,0.25)	Ba	4*d* (0,0.5,0.25)
x	0.4989(5)	*x*	0.2506(1)	*x*	0.2502(1)	*B* (Å)^2	0.29(2)	*B* (Å)^2	0.38(2)
z	0.2516(3)	*B* (Å)^2	0.95(5)	*B* (Å)^2	0.99(4)	Ca	2*a* (0,0,0)	Ca	2*a* (0,0,0)
B (Å)^2	0.44(3)	Sr	1*a* (0,0,0)	Sr	1*a* (0,0,0)	*B* (Å)^2	0.27(6)	*B* (Å)^2	0.42(7)
Sr	2*c* (0.5,0,0)	*B* (Å)^2	0.68(7)	*B* (Å)^2	0.64(7)	W	2*b* (0,0,0.5)	W	2*b* (0,0,0.5)
B (Å)^2	0.81(4)	Te	1*b* (0.5,0.5,0.5)	Te	1*b* (0.5,0.5,0.5)	*B* (Å)^2	0.06(1)	*B* (Å)^2	0.12(1)
W	2*b* (0,0.5,0)	*B* (Å)^2	0.05(3)	*B* (Å)^2	0.10(3)	O(1)	4*e* (0,0,*z*)	O(1)	4*e* (0,0,*z*)
B (Å)^2	0.25(3)	O	6*f* (*x*,*y*,*z*)	O	6*f* (*x*,*y*,*z*)	*z*	0.267(1)	*z*	0.274(2)
O(1)	4*i* (*x*,0,*z*)	*x*	−0.218(2)	*x*	−0.279(2)	*B* (Å)^2	0.3(1)	*B* (Å)^2	0.3(1)
x	0.553(2)	*z*	0.226(2)	*z*	0.223(2)	O(2)	8*h*(*x*,*y*,0)	O(2)	8*h*(*x*,*y*,0)
z	0.279(2)	*z*	0.334(2)	*z*	0.333(2)	*x*	0.242(1)	*x*	0.238(2)
B (Å)^2	0.62(4)	*B* (Å)^2	2.3(2)	*B* (Å)^2	2.6(3)	*y*	0.302(1)	*y*	0.299(2)
O(2)	8*j* (*x*,*y*,*z*)					*B* (Å)^2	0.3(1)	*B* (Å)^2	0.3(1)
x	0.2109(4)								
y	0.2573(6)								
z	0.0429(3)								
B (Å)^2	0.89(8)								
R_{wp} = 8.36%		R_{wp} = 8.75%		R_{wp} = 8.59%		R_{wp} = 10.94%		R_{wp} = 11.15%	
R_p = 6.49%		R_p = 6.68%		R_p = 6.56%		R_p = 8.08%		R_p = 8.28%	

Table 3
Selected interatomic distances (Å) in $Ba_2MM'O_6$ (M = Sr, Ca, M' = U, W, Te) at room temperature

	Ba_2SrWO_6	Ba_2SrTeO_6	Ba_2CaUO_6	Ba_2CaWO_6	Ba_2CaTeO_6
M–O(1)	2.402(5) 2 ×	2.328(7) 6 ×	2.289(12) 2 ×	2.223(4) 6 ×	2.241(5) 6 ×
M–O(2)	2.414(3) 4 ×		2.296(14) 2 ×		
M–O(3)			2.356(12) 2 ×		
M'–O(1)	1.935(5) 2 ×	1.988(7) 7 ×	2.115(13) 2 ×	1.974(4) 6 ×	1.957(5) 6 ×
M'–O(2)	1.920(2) 4 ×		2.079(15) 2 ×		
M'–O(3)			2.072(10) 2 ×		
Ba–O(1)	2.717(5) 1 ×	2.821(4) 4 ×	2.734(16) 1 ×	2.9703(3) 12 ×	2.9713(2) 12 ×
	3.0553(8) 2 ×	3.031(13) 4 ×	2.975(21) 1 ×		
	3.407(5) 1 ×	3.275(4) 4 ×	3.121(22) 1 ×		
			3.476(16) 1 ×		
Ba–O(2)	2.816(3) 2 ×		2.834(17) 1 ×		
	2.831(3) 2 ×		2.942(16) 1 ×		
	3.239(3) 2 ×		3.141(17) 1 ×		
	3.290(3) 2 ×		3.369(17) 1 ×		
Ba–O(3)			2.639(8) 1 ×		
			2.957(11) 1 ×		
			3.247(12) 1 ×		
			3.536(8) 1 ×		

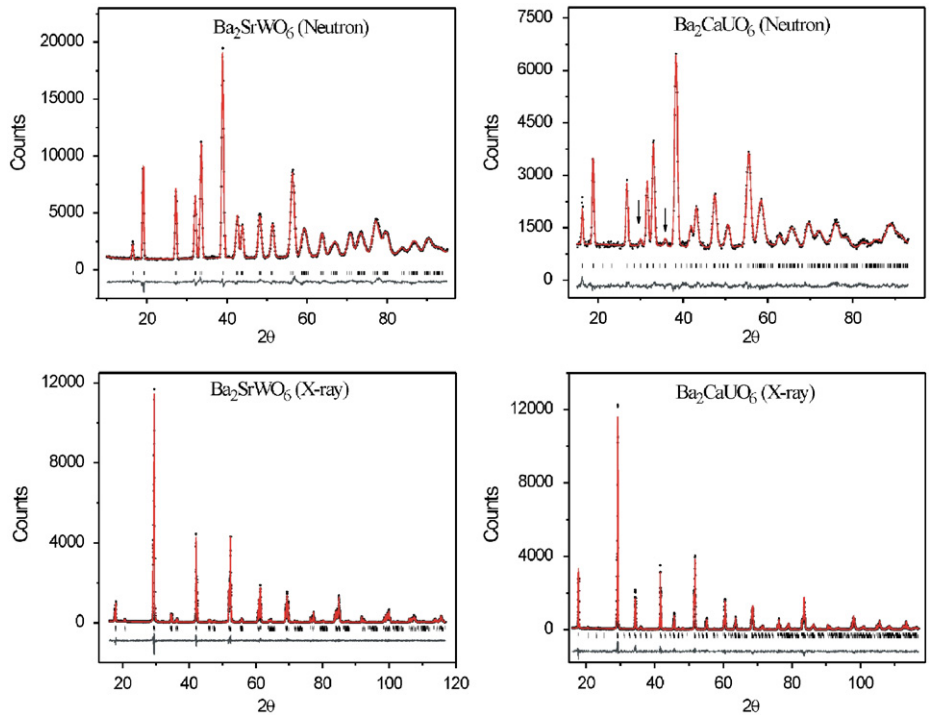

Fig. 4. Observed (crosses) and calculated (full line) profiles of the neutron and the X-ray powder diffraction for Ba_2SrWO_6 and Ba_2CaUO_6, respectively. Tick marks below the profiles indicate the positions of the allowed Bragg reflections. A difference curve (observed–calculated) is shown at the bottom of each plot. Note that some superlattice reflections due to in-phase octahedral tilt in Ba_2CaUO_6 are indicated by arrows.

rhombohedral angle decreases quasi-linearly with increasing T [29], the transition temperature of the continuous $R\bar{3} \rightarrow Fm\bar{3}m$ phase transition in Ba_2SrWO_6 is expected to occur at about above 1300 K.

4.2. Ba_2SrTeO_6

Unlike the previously reported tetragonal symmetry [19], Ba_2SrTeO_6 adopts the rhombohedral space group $R\bar{3}$. This structure consists of the tilting of the octahedra around the [111]-axis of the cubic aristotype. As was mentioned in Section 1, our earlier investigations on the Ba_2LnMO_6-type double perovskites showed two possible structures, i.e. $I4/m$ ($a^0a^0c^-$) or $R\bar{3}$ ($a^-a^-a^-$), existing between the $I2/m$ and $Fm\bar{3}m$ structures. It was further suggested that the preference of one tilt system over the other may depend on the covalency of the octahedral M-cation. For example, Nb is more electropositive and some members of Ba_2LnNbO_6, e.g. Ln = Eu, Gd, Tb, and Dy, adopt the tetragonal $I4/m$ structure. For double perovskites that contain less electropositive cations, such as Ru, Ir, Sb, and Bi, the rhombohedral $R\bar{3}$ structure is preferred. Tellurium is clearly more electronegative and the occurrence of rhombohedral symmetry in Ba_2SrTeO_6 is in agreement with this suggestion.

It should be noted that the tolerance factor of Ba_2SrTeO_6 ($t = 0.938$) deviates significantly from unity, but it retains the rhombohedral symmetry. This is in contrast to the series of Ba_2LnNbO_6 [12] and Ba_2LnBiO_6 [28], in which the monoclinic $I2/m$ structure is seen when the tolerance factors are roughly less than 0.968 and 0.950, respectively. The particularly stable rhombohedral symmetry in Ba_2SrTeO_6 is attributed to the more covalent nature of the Te–O bonds. As was shown by Woodward [32], the rhombohedral $a^-a^-a^-$ tilt system results, when compared to other tilt systems (e.g. the monoclinic $a^0b^-b^-$), in the highest coulomb attraction between the ions, but it maximizes the repulsive energy too. Therefore, if the ionic contribution of the *A*-cation is large, the rhombohedral structure is favoured because the attractive term overweighs the repulsive one. As was argued previously [12,25], the increase of covalency at the octahedral site may strengthen the ionic contribution of large cations to the total energy, favoring thus the rhombohedral structure. This trend can also be seen in the double perovskite Ba_2BiTaO_6 [33]. Despite the relatively small value of the tolerance factor ($t = 0.952$), this compound adopts the rhombohedral structure as a result of a quite covalent Bi–O bonding.

It is worth mentioning that among the known rhombohedral $Ba_2M(II)M'(VI)O_6$ double perovskites, only Ba_2SrIrO_6 was reported to have the space group $R\bar{3}m$ [14]. This space group does not actually belong to Glazer's tilt systems [6,8] and contains no octahedral tilting. However, since $R\bar{3}m$ has the same reflection conditions as $R\bar{3}$ ($a^-a^-a^-$), it may be difficult to distinguish experimentally between the two space groups. For instance, the space group $R\bar{3}m$ was once assigned to Ba_2BiSbO_6 based on the single-crystal X-ray diffraction data [34], but later investigation using neutron powder diffraction technique showed $R\bar{3}$ being the correct space group [35]. In the light of the present investigation, the space group $R\bar{3}m$ reported for Ba_2SrIrO_6 may be incorrect if the rhombohedral distortion in this double perovskite is resulted from the octahedral tilting.

4.3. Ba_2CaUO_6

The present study confirms the earlier finding that Ba_2CaUO_6 is non-cubic [21], but differs with the orthorhombic description of Kemmler-Sack and Seemann [20]. As was clearly revealed in Fig. 1, the basic (222) reflection splits in a triplet. In an orthorhombic cell with the dimension of $a \approx b \approx \sqrt{2}a_p$ and $c \approx 2a_p$, this reflection would be a doublet. In fact, among the space groups derived from the octahedral tilting in ordered double perovskites, only *Pnnn* belongs to the orthorhombic system [6,8]. Nevertheless, this space group does not allow the the (222) reflection to split. On the other hand, the monoclinic distortion in Ba_2CaUO_6 is relatively small as can be seen from the refined monoclinic angle (Table 1). This possibly explains why an orthorhombic cell was previously found for this compound [20].

In Ba_2CaUO_6, the octahedra tilt both about the two-fold [110] (out-of-phase) and about the four-fold [001]-axis (in-phase) of the cubic aristotype, with the averaged tilting angles of 9.9° and 4.9°, respectively. Although the tilt system ($a^-a^-c^+$) is often observed in $Sr_2MM'O_6$-type double perovskites [36], in those containing Ba-cation only Ba_2SrUO_6 ($t = 0.904$) is, to the best of our knowledge, known to adopt the $P2_1/n$ structure at room temperature [13]. Given a tolerance factor of 0.940, the observed tilt system in Ba_2CaUO_6 is somewhat unexpected: Ba_2SrWO_6, which has an even smaller value of the tolerance factor ($t = 0.929$), adopts the space group $I2/m$. However, a close examination shows that the unit cell dimension of Ba_2CaUO_6 is even larger than that of Ba_2SrWO_6 (see Fig. 1 and Table 1), despite that the averaged ionic radius of Ca(II) and U(IV) (0.865 Å) is smaller than that of Sr(II) and W(VI) (0.890 Å). The reason for this is not clear but could be due to a different compressibility of the low-charge *M*-cation in double perovskites. It has been shown earlier [11] that in $Ba_2Ln(III)M(V)O_6$-type double perovskites, the (averaged) *Ln*(III)–O bond lengths are actually shorter than those estimated from the sum of the corresponding ionic radii [37]; but that of *M*(V)–O agrees generally well with the sum of ionic radii. This is not surprising since the *Ln*(III)-cation is bigger than the *M*(V)-cation. The size reduction of the LnO_6 octahedron to some extend would not affect the anion–anion repulsion. This is also the case in the systems discussed in this paper. For example, in Ba_2SrWO_6 and Ba_2CaWO_6 (see also discussion below); the averaged Sr–O (~2.41 Å) and Ca–O (2.22 Å) bond lengths (Table 3) are significantly shorter than the predicted values (2.58 and 2.40 Å, respectively) [37]. On the other hand, we noticed that the shortening of the Ca–O bond lengths in Ba_2CaUO_6 (the averaged value 2.31 Å) is less than that in Ba_2CaWO_6. Also in Ba_2SrUO_6 [13], the averaged Sr–O bond length (2.46 Å) is somewhat larger than that in Ba_2SrWO_6. Apparently, the ease of having short *M*–O bond distances depends on the nature of *M'*-cation: the more covalent *M'*-cation is, the shorter the *M*–O bond length is. This may be understood from the fact that the covalent cation has lower effective charge, which reduces the cation–cation repulsion. Uranium is more electropositive than tungsten; the relative change in size of the alkaline earths is smaller in uranates than in tungstates. This trend can also be seen in Ba_2LaSbO_6 [11] and Ba_2LaNbO_6 [12]. The averaged La–O bond distances are 2.342 and 2.379 Å, being approximately 4% and 2% shorter than the sum of ionic radii (2.432 Å), which is attributable to the more electronegative nature of Sb. Clearly, the tolerance factors obtained from the normal ionic radii cannot be used indiscriminately to prejudge the structure of the distorted double perovskites.

In Table 4, the lattice constants of some known double perovskites containing alkaline earth and actinide cations are compared. Gens et al. [21] described Ba_2CaMO_6 (M = Np, Pu) as cubic and Ba_2SrMO_6 (M = Np, Pu) as orthorhombic. They also indicated that the true symmetry of these compounds could be lower. Based on the present investigation, the structure of these double perovskites is expected to be isomorphic to the uranates with the space group $P2_1/n$.

4.4. Ba_2CaWO_6 and Ba_2CaTeO_6

Both Ba_2CaWO_6 and Ba_2CaTeO_6 are found to be cubic with the space group $Fm\bar{3}m$. Considering their tolerance factors (0.967 and 0.976, respectively), the occurrence of cubic structure in these compounds is somewhat unexpected. As was mentioned above, the *M*–O bond lengths of the low charge cation can be significantly shorter than those estimated from the sum of the ionic radii. This makes the tolerance factor inadequate to predict the distortion in double perovskites. For example, the cubic structure is seen in some members of $Ba_2M(III)M'(V)O_6$ (M = lanthanides and Y and M' = Ru, Ir, Sb, and Nb) [9–12], with

Table 4
Lattice parameters and the tolerance factors of some double perovskites containing actinides

	a (Å)	*b* (Å)	*c* (Å)	*β* (deg)	*t*	Reference
Ba_2CaUO_6	6.15912 (6)	6.11638 (7)	8.6441 (1)	89.8994 (8)	0.940	This work
Ba_2CaNpO_6	8.6235 (3)				0.942	[21]
Ba_2CaPuO_6	8.6112 (2)				0.944	[21]
Ba_2SrUO_6	6.2501 (4)	6.2697 (4)	8.8355 (6)	89.760 (8)	0.904	[9]
Ba_2SrNpO_6	6.221 (4)	6.215 (6)	8.863 (3)		0.906	[21]
Ba_2SrPuO_6	6.204 (4)	6.188 (6)	8.882 (3)		0.908	[21]

t-values being about 0.98. Also in Ba_2CaReO_6 ($t = 0.979$) and Ba_2CaOsO_6 ($t = 0.98$) [24], the space group $Fm\bar{3}m$ is observed. Clearly, in double perovskites the apparent mismatch between A–O and the averaged M/M'–O bond lengths can be suppressed by shortening the M–O bond distances without necessarily tilting the $M/M'O_6$ octahedra.

As noted before, Yamamura et al. [24] have observed, from the specific heat measurement, a second-order phase transition in Ba_2CaWO_6 at $T \approx 220$ K. They assigned the phase transition as corresponding to $I4/m \rightarrow I2/m$ transition. However, such description cannot be correct, since there is no pathway that allows a continuous change between the tilt systems $a^0a^0c^-$ ($I4/m$) and $a^0b^-b^-$ ($I2/m$). The $I4/m \rightarrow I2/m$ phase transition must be first order in nature. As was shown in the present investigation, the cubic structure of Ba_2CaWO_6 transforms to the tetragonal structure at the temperature below about 240 K (Fig. 3). Since the transition between the tilt systems $a^0a^0a^0$ and $a^0a^0c^-$ is continuous, the second-order phase transition observed by Yamamura et al. is likely to be $Fm\bar{3}m \rightarrow I4/m$.

In conclusion, we have studied the crystal structures of several double perovskites in $Ba_2M(II)M'(VI)O_6$ (M = Sr and Ca; M' = Te, W, and U) to look for the relationship between the tilt systems and the tolerance factors. In the case of M = Sr, the space groups at room temperature are $R\bar{3}$ ($a^-a^-a^-$), $I2/m$ ($a^0b^-b^-$) and $P2_1/n$ ($a^-a^-c^+$) for M' = Te, W, and U, which is expected when the ionic radius of the M' = cations increases (0.56, 0.60, and 0.73 Å, respectively). Also, the occurrence of $Fm\bar{3}m$ ($a^0a^0a^0$) and $P2_1/n$ ($a^-a^-c^+$) structures in $Ba_2CaM'O_6$ (M' = Te, W, and U) reflects such general trend. However, a suitable tilt system for a given double perovskite may depend critically on the nature of octahedral cations. For example, in $Ba_2MM'O_6$-type double perovskites, the rhombohedral tilt system $a^-a^-a^-$, as compared to the tetragonal $a^0a^0c^-$, is favored by more covalent M/M'-cations. If covalency is high (e.g. Ba_2SrTeO_6), the rhombohedral structure may be as stable as against the monoclinic tilt system ($a^0b^-b^-$), despite a large deviation of the tolerance factor. In addition, the cubic structure can be stabilized in double perovskites by compressing the low charge of M-cations to actually adjust the matching between A–O and M/M'–O bond lengths instead of tilting the normally rigid $M/M'O_6$ octahedra. This is particularly true when the covalency of the M'-cation is high. Finally, the rhombohedral $R\bar{3}$ structure was observed in Ba_2SrWO_6 above room temperature before becoming cubic, and the continuous phase transition in Ba_2CaWO_6 below room temperature was identified to be $Fm\bar{3}m \rightarrow I4/m$.

Acknowledgments

The authors are indebted to Mr. A. Bontenbal of NRG, Petten, The Netherlands, for the collection of the neutron powder diffraction data and to Dr. R.A.G. de Graaff for valuable discussions.

References

[1] A.W. Sleight, J.L. Gillson, P.E. Bierstedt, Solid State Commun. 17 (1975) 27.
[2] D.E. Cox, A.W. Sleight, in: R.M. Moon (Ed.), Proceedings of the Conference on Neutron Scattering, Gatlinburg, Nat. Techn. Info Service, Springfield, VA, 1976, p. 45.
[3] M.A. Akbas, P.K. Davies, J. Am. Ceram. Soc. 81 (1998) 670.
[4] I.M. Reaney, E.L. Colla, N. Setter, Jpn. J. Appl. Phys. 33 (1994) 3984.
[5] K.-I. Kobayashi, T. Kimura, H. Sawada, K. Terakura, Y. Tokura, Nature (London) 395 (1998) 677.
[6] P.M. Woodward, Acta Crystallogr. B 53 (1997) 32.
[7] A.M. Glazer, Acta Crystallogr. A 31 (1975) 756.
[8] C.J. Howard, B.J. Kennedy, P.M. Woodward, Acta Crystallogr. 59 (2003) 463.
[9] W.T. Fu, D.J.W. IJdo, J. Alloys Compds. 394 (2005) L5.
[10] W.T. Fu, D.J.W. IJdo, Solid State Commun. 136 (2005) 456.
[11] W.T. Fu, D.J.W. IJdo, J. Solid State Chem. 178 (2005) 2363.
[12] W.T. Fu, D.J.W. IJdo, J. Solid State Chem. 179 (2006) 1022.
[13] W.A. Groen, D.J.W. IJdo, Acta Crystallogr. C 43 (1987) 1033.
[14] D.-Y. Jung, P. Gravereau, G. Demazeau, Eur. J. Solid State Inorg. Chem. 30 (1993) 1025.
[15] E.G. Steward, H.P. Rooksby, Acta Crystallogr. 4 (1951) 503.
[16] L.M. Kovba, L.N. Lykova, N.N. Shevchenko, Russ. J. Inorg. Chem. 15 (1971) 1150.
[17] D.E. Cox, J.B. Hastings, W. Thomlinson, Acta Crystallogr. A 40 (1984) C368.
[18] D.D. Khalyavin, A.M.R. Senos, P.Q. Mantas, Powder Diffraction 19 (2004) 280.
[19] N. Külcü, M. Trömel, J. Appl. Cryst. 17 (1984) 456.
[20] S. Kemmler-Sack, I. Seemann, Z. Anorg. Allg. Chem. 411 (1975) 61.
[21] R. Gens, J. Fuger, L.R. Mors, C.W. Williams, J. Chem. Thermodyn. 17 (1985) 561.
[22] V.S. Filip'ev, G.E. Shatalova, E.G. Fesenko, Kristallografiya 19 (1974) 386.
[23] N.S. Chi, S.H. Bauer, Acta Crystallogr. C 40 (1984) 1646.
[24] K. Yamamura, M. Wakeshima, Y. Hinatsu, J. Solid State Chem. 179 (2006) 609.
[25] W.T. Fu, S. Akerboom, D.J.W. IJdo, J. Solid State Chem. 180 (2007) 1547.
[26] C.J. Howard, B.A. Hunter, A Computer Program for Rietveld Analysis of X-ray and Neutron Powder Diffraction Patterns, Lucas Height Research Laboratories, 1998.
[27] D.E. Cox, A.W. Sleight, Solid State Commun. 19 (1976) 969.
[28] W.T. Harrison, K.P. Reis, A.J. Jacobson, L.F. Schneemeyer, J.V. Waczak, Chem. Mater. 7 (1995) 2161.
[29] P.J. Saines, J.R. Spencer, B.J. Kennedy, Y. Kubotab, C. Minakata, H. Hano, K. Kato, M. Takata, J. Solid State Chem. 180 (2007) 3001.
[30] W.T. Fu, D. Visser, K.S. Knight, D.J.W. IJdo, J. Solid State Chem. 177 (2004) 1667.
[31] R.B. Macquart, B.J. Kennedy, Chem. Mater. 17 (2005) 1905.
[32] P.M. Woodward, Acta Crystallogr. B 53 (1997) 44.
[33] K.S. Wallwork, B.J. Kennedy, Q. Zhou, Y. Lee, T. Voigt, J. Solid State Chem. 178 (2005) 207.
[34] W.T. Fu, R. de Gelder, R.A.G. de Graaff, Mater. Res. Bull. 32 (1997) 657.
[35] W.T. Fu, Solid State Commun. 116 (2000) 461.
[36] M.W. Lufaso, P.W. Barnes, P.M. Woodward, Acta Crystallogr. B 62 (2006) 397.
[37] R.D. Shannon, Acta Crystallogr. A 32 (1976) 751.